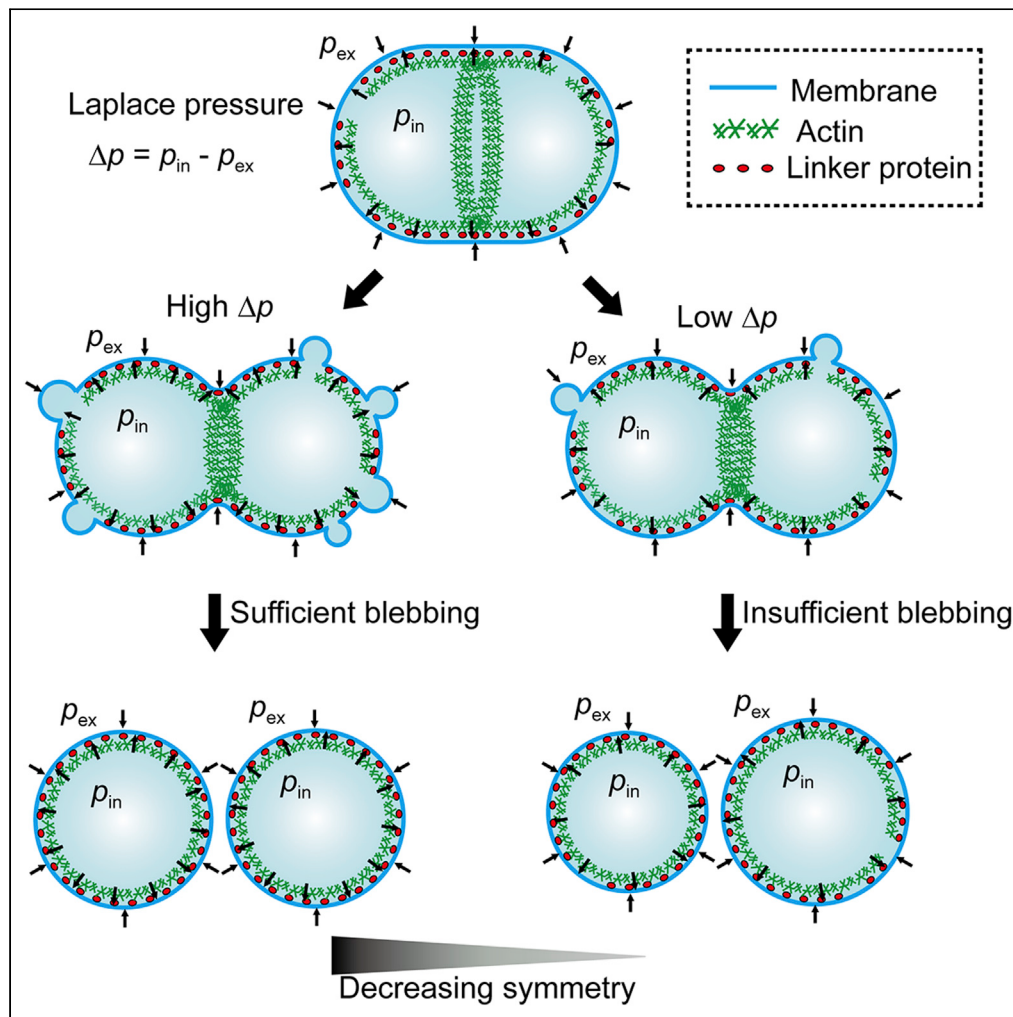


## Article

## Effects of the Laplace pressure on the cells during cytokinesis



Xiaohuan Wang,  
Long Li, Yingfeng  
Shao, ..., Songjie  
Zheng, Yuqiao Li,  
Fan Song

songf@lnm.imech.ac.cn

**Highlights**

The Laplace pressure controls the distribution and size of cell blebbing

The Laplace pressure helps to develop a more uniform cell boundary

The Laplace pressure regulates symmetry of cell division by way of blebs



## Article

## Effects of the Laplace pressure on the cells during cytokinesis

Xiaohuan Wang,<sup>1,2,4</sup> Long Li,<sup>1,4</sup> Yingfeng Shao,<sup>1</sup> Jiachen Wei,<sup>1</sup> Ruopu Song,<sup>3</sup> Songjie Zheng,<sup>1,2</sup> Yuqiao Li,<sup>1,2</sup> and Fan Song<sup>1,2,5,\*</sup>

## SUMMARY

The Laplace pressure is one of the most fundamental regulators that determine cell shape and function, and thus has been receiving widespread attention. Here, we systematically investigate the effect of the Laplace pressure on the shape and function of the cells during cytokinesis. We find that the Laplace pressure during cytokinesis can directly control the distribution and size of cell blebbing and adjust the symmetry of cell division by virtue of changing the characteristics of cell blebbing. Further, we demonstrate that the Laplace pressure changes the structural uniformity of cell boundary to regulate the symmetry of cell division. Our findings provide further insights as to the important role of the Laplace pressure in regulating the symmetry of cell division during cytokinesis.

## INTRODUCTION

The Laplace pressure of the cells, which is the difference between intracellular and extracellular pressures, is generated by water fluxion caused by cell osmolarity change or cortex contraction (Stewart et al., 2011; Strychalski and Guy, 2016). Note that the Laplace pressure, as originally defined by the Young-Laplace equation, is the pressure difference between the inside and the outside of a curved surface that forms the gas/liquid boundary and results from the surface tension of the gas/liquid interface (Butt et al., 2013). Here, we use the term of Laplace pressure to signify the hydrostatic pressure difference across the membrane. As a transmembrane pressure, the Laplace pressure is demonstrated not only to be a mechanical regulator that can rapidly reassign the cell shape and behavior (Chengappa et al., 2018) and to span at least two orders of magnitude (Petrie and Koo, 2014; Stewart et al., 2011; Yanai et al., 1996), but also to play a key role in various cellular processes, including cell migration (Wehner et al., 2003; Yanai et al., 1996), proliferation (Cayley and Record, 2003), necrosis and apoptosis (Guan et al., 2006; Lang et al., 2005), as well as the material transportation and the signal transduction (Le Bihan et al., 2006; Li et al., 2020). Particularly, each cell during mitosis goes through a simple and dramatic shape change process (Reichl et al., 2005; Zhang and Robinson, 2005), and the Laplace pressure in the process undergoes more than a 10-fold change (Sorce et al., 2015). For example, the elevated Laplace pressure induced by increased intracellular osmolarity is the main cause of cell rounding at mitotic entry (Stewart et al., 2011); after that, the constriction of both the contractile ring and the polar cortex during cytokinesis contribute to the increase of the Laplace pressure (Sedzinski et al., 2011), which is deemed to functionally play a dual role: acting as resistance force to antagonize the contractile ring early in cytokinesis while helping to drive furrow ingression late in cytokinesis (Zhang and Robinson, 2005). However, despite the increasing appreciation of physiological significance of this transmembrane pressure, the effects of the Laplace pressure on the cytokinesis process have been still poorly understood so far.

The Laplace pressure during cytokinesis, on the one hand, drives cell blebbing, which is a prominent cellular and highly dynamic behavior in mitosis (Charras et al., 2008), as well as migration (Charras and Paluch, 2008). The blebs caused by the Laplace pressure are the plasma membrane protrusions on the cortex-membrane boundary of the cells and occur at the sites with cortex defects or missing linker proteins in the boundary (Charras and Paluch, 2008; Charras et al., 2006). Blebbing is a common feature of cell physiology during cytokinesis (Charras, 2008; Charras et al., 2008) and has been observed in, but not limited to, HeLa cell (Sedzinski et al., 2011), L929 cell (Sedzinski et al., 2011), BSC1 cell (Boucrot and Kirchhausen, 2007), Swiss 3T3 fibroblast (Burton and Taylor, 1997), NRK cell (Fishkind et al., 1991), BHK21 cell (Erickson and Trinckaus, 1976). For the migration of a cell, high pressure triggers protrusions to form the lobopodia while low pressure produces lamellipodia (Petrie and Koo, 2014). For the mitosis of a cell, however, the biological

<sup>1</sup>State Key Laboratory of Nonlinear Mechanics and Beijing Key Laboratory of Engineered Construction and Mechanobiology, Institute of Mechanics, Chinese Academy of Sciences, Beijing 100190, China

<sup>2</sup>School of Engineering Science, University of Chinese Academy of Sciences, Beijing 100049, China

<sup>3</sup>School of Life Science and Health, Northeastern University, Shenyang 110169, China

<sup>4</sup>These authors contributed equally

<sup>5</sup>Lead contact

\*Correspondence:  
song@lnm.imech.ac.cn

<https://doi.org/10.1016/j.isci.2021.102945>



significance of cell blebbing has not been completely understood up to now. The existing studies indicate that the life cycle of a bleb consists of bleb initiation, bleb expansion, cortex reassembly, and retraction ([Charras and Paluch, 2008](#)). The bleb initiation begins under a proper Laplace pressure when there is a local defect in the cortex-membrane boundary, while the boundary can restore to a normal state after the cell cortex reassembly and bleb retraction under another proper Laplace pressure ([Alert and Casademunt, 2016](#)). Obviously, the whole bleb evolving processes during cytokinesis are associated intimately with the change of the Laplace pressure. So, we believe that the Laplace pressure has a fundamental biological significance on the cell blebbing during cytokinesis.

On the other hand, the change of the Laplace pressure can lead to the cytoplasmic oscillation inside the cells during cytokinesis. Specifically, the difference between the pressures generated by the different membrane tension of the two poles of the cells gives rise to the back and forth flow of the cytoplasm between the two poles, which is also related closely to the cell blebbing at the two poles ([Sedzinski et al., 2011](#)). Recent investigations demonstrate that the high Laplace pressure intrinsically puts the cells during cytokinesis in an unstable state that may cause uncontrolled cytoplasmic oscillations and may finally result in asymmetric division or division failure ([Dorn and Maddox, 2011](#); [Sedzinski et al., 2011](#)). Obviously, the Laplace pressure is associated with the size symmetry of cell division which determines the activity and vitality of the newborn daughter cells. However, the effect of the Laplace pressure on cell division has been hardly understood yet. Although the symmetry of cell division is traditionally deemed to be determined by anaphase spindle, which releases signals to designate the site for the contractile ring assembly and thus determines the cleavage plane ([Grill et al., 2003](#); [Kiyomitsu, 2015](#); [Sansregret and Petronczki, 2013](#)), we have reason to speculate that the Laplace pressure can effectively affects the size symmetry of cell division.

In this paper, by controlling the extracellular osmolarity to adjust the intracellular pressures of the cells, thus, to regulate their Laplace pressures, we systematically investigate the effects of the Laplace pressure on the shape and behavior of the cells during cytokinesis. We demonstrate that (i) abruptly changing the Laplace pressure of the cells results in the geometrically self-similar change of cell shape, thus, a cytokinesis factor is defined to characterize the real-time shape of a dividing cell; (ii) change to the Laplace pressure of the cells induces the changes of the distribution and size of cell blebbing: the higher the Laplace pressure is, the greater the proportion of the blebbing in the earlier stage is, and the sooner the blebbing activity completes; (iii) change to the Laplace pressure of the cells changes the symmetry via cell blebbing; (iv) the sufficient accomplishment of cell blebbing directly promotes the size symmetry of cell division, which highlights the biological significance of the cell blebbing in mitosis; (v) change in the Laplace pressure affects the structure of the cortex, which constitutes the mechanism that the change of the Laplace pressure can change the cell blebbing and division in mitosis; and (vi) the size symmetry of cell division is substantially determined by the uniformity of cell cortex-membrane boundary. These results contribute to a deeper understanding of the essential role of the Laplace pressure in cellular life processes.

## RESULTS AND DISCUSSION

To investigate the effects of the Laplace pressures of the cells on their shape and behavior changes from cleavage furrow emergence to contractile-ring contraction accomplishment, we control the extracellular osmolarities to adjust the intracellular pressures, thus, to regulate their Laplace pressures. In the experiments, once the cleavage furrows of the tested cells just emerge, the isotonic media in which the cells are being normally cultured are rapidly replaced by the tested media with different osmolarities. Specifically, using micropipette aspiration technique, we measure the change of the Laplace pressure of cells in respond to hypotonic or hypertonic shocks when cells just enter into cytokinesis. As shown in [Figure 1A](#), the Laplace pressure, which is measured to be  $236 \pm 57$  Pa ( $n = 8$ ) in isotonic medium, increases by about 39% and 20% in the hypotonic media with 180 and 240 mOsm/kg, respectively, and decreases by about 50% and 74% in the hypertonic media with 360 and 420 mOsm/kg, respectively. Evidently, the Laplace pressure of a cell decreases with the extracellular osmolarity.

### Changing the Laplace pressure triggers the geometrically self-similar change of cell shape

When the isotonic media with 300 mOsm/kg in which the tested cells are normally cultured are rapidly replaced by the media with the different osmolarities that can effectively keep the tested cells undergoing physiologically normal cytokinesis ([Kim and Lee, 2002](#); [Oldenhofer et al., 2011](#)), we observe that all the cells during cytokinesis roughly undergo swelling in the hypotonic media with 180 and 240 mOsm/kg and shrinkage in the hypertonic media with 360 and 420 mOsm/kg in a geometrically self-similar way within

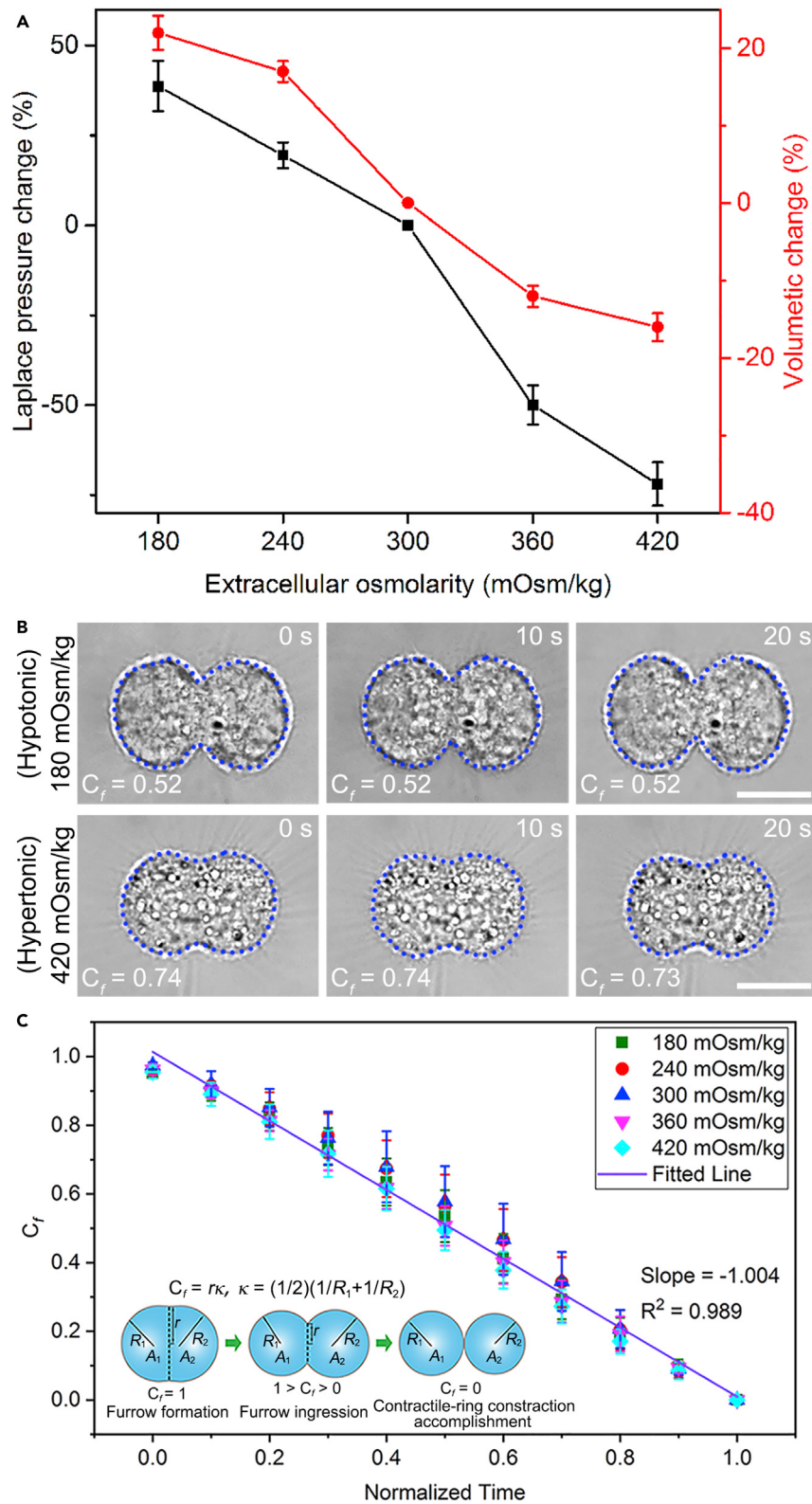


**Figure 1. The change of the Laplace pressure and its effect on the cell volume and shape**

(A) The change of the Laplace pressure and volume for the cells undergoing cytokinesis in response to the osmotic shocks. Error bars are SDs.

(B) Snapshots of the shape changes of the cells during cytokinesis in the initial 20 s after media replacement: the cells swell in the hypotonic media and shrink in the hypertonic media in a geometrically self-similar way within initial 20 s. The blue dashed lines outline the boundaries of the cells. The numbers in the upper right and lower left of the panels indicate recording time (the moment of solution exchange corresponds to 0 s) and the real-time values of the cytokinesis factor  $C_f$ , respectively. Scale bars, 10  $\mu\text{m}$ .

(C) The changes of  $C_f$  for the cells undergoing cytokinesis in the media with different osmolarities. The horizontal axis denotes the time normalized by dividing by the cytokinesis time of each cell. The purple solid line is the fitted line of the experimental data, and its slope and the coefficient of determination ( $R^2$ ) are shown in the lower right. Error bars are SDs. The inset in the lower left illustrates the definition of  $C_f$ , where  $R_1$  and  $R_2$  are the real-time effective radii of the two forming daughter cells, respectively, and obtained by real-timely measuring the cross-sectional areas of the two forming daughter cells,  $A_1$  and  $A_2$ .

initial 20 s, and then, continue their unfinished cytokinesis process in the tested media (Figure 1B). By real-time measurements, we find that the mean volume of the cells swell by about 22% and 17% in the hypotonic media with 180 and 240 mOsm/kg, respectively, and the mean volume of the cells shrink by about 12% and 16% in the hypertonic media with 360 and 420 mOsm/kg, respectively (Figure 1A). This is an indication that the volumetric change of a cell decreases with the change of its extracellular osmolarities. Together, results of Figure 1A indicate a positive correlation between the change of the Laplace pressures of the cell and its volumetric change.

Further, we find that the ratio of the mean curvature of the two forming daughter cells,  $\kappa = (1/2)(1/R_1 + 1/R_2)$ , to the curvature of the cleavage furrow,  $1/r$ , changes independently with the extracellular osmolarity and reduces linearly from 1 to 0 when the cells evolve from cleavage furrow emergence to contractile-ring contraction accomplishment, where  $R_1$  and  $R_2$  are the real-time effective radii of the two forming daughter cells, respectively, and  $r$  is the real-time radius of the cleavage furrow (Figure 1C). So, we can define  $C_f = r\kappa$  as a cytokinesis factor to characterize the real-time shape of a cell during cytokinesis. Obviously, in the process of the symmetric cell division  $C_f$  is just the ratio of the radii of the cleavage furrow and the forming daughter cells. Specifically,  $C_f = 1$  signifies the onset of cytokinesis.  $C_f$  decreases from 1 to 0 with the ingress of the cleavage furrow. When the contractile-ring contraction completes,  $C_f = 0$ .

**Change to the Laplace pressure induces the changes of the distribution and size of cell blebbing**

In the process of  $C_f = 1-0$ , lots of blebs are observed to occur at the surfaces of all the cells in the tested media with the different osmolarities (Figures 2A, S1; Videos S1, S2, S3, S4, and S5). However, we find that both the cell blebbing distributions and sizes rely intimately on the extracellular osmolarities. Further, the statistical results indicate that with the elevation of extracellular osmolarity, the blebbing number and size of the cells monotonously increase and decrease, respectively (Figure 2B). Note that, the actomyosin contractility also contributes to increasing the Laplace pressure during cytokinesis (Charras et al., 2008; Sao et al., 2019). For this reason, blebs also occur even for cells undergoing cytokinesis in isotonic and hypertonnic media.

To obtain the distribution law of the cell blebbing, the whole process of  $C_f$  is divided into five equal stages based on  $C_f$  values. In the hypotonic medium with the extracellular osmolarity of 180 mOsm/kg, more than 77% of all the blebs occur in the early stage,  $C_f = 1-0.8$ ; in the isotonic medium with 300 mOsm/kg, the peak value of the blebbing proportion, about 31%, occurs in the middle stage,  $C_f = 0.6-0.4$ ; and in the hypertonic medium with 420 mOsm/kg, the peak value, about 32%, occurs in the late stage,  $C_f = 0.2-0$  (Figure 2C). Therefore, with the increase of the extracellular osmolarity, the peak value of cell blebbing proportion gradually shifts from early to late stages of cytokinesis. This is an indication that the distribution of the cell blebbing during cytokinesis varies with the change of the Laplace pressure: the lower the extracellular osmolarity, i.e. the higher the Laplace pressure, the greater the proportion of the blebbing in the earlier stage.

Particularly, we find that after  $C_f = 0$ , cell blebbing is hardly observed at the surfaces of the newborn daughter cells in the hypotonic media. However, some blebs generated in the late stage still remain at the surfaces of the newborn daughter cells in the isotonic and hypertonic media (Column 7 and Rows 3-5 of Figure 2A). The residual blebs can automatically fade away within tens of seconds after  $C_f = 0$ , which

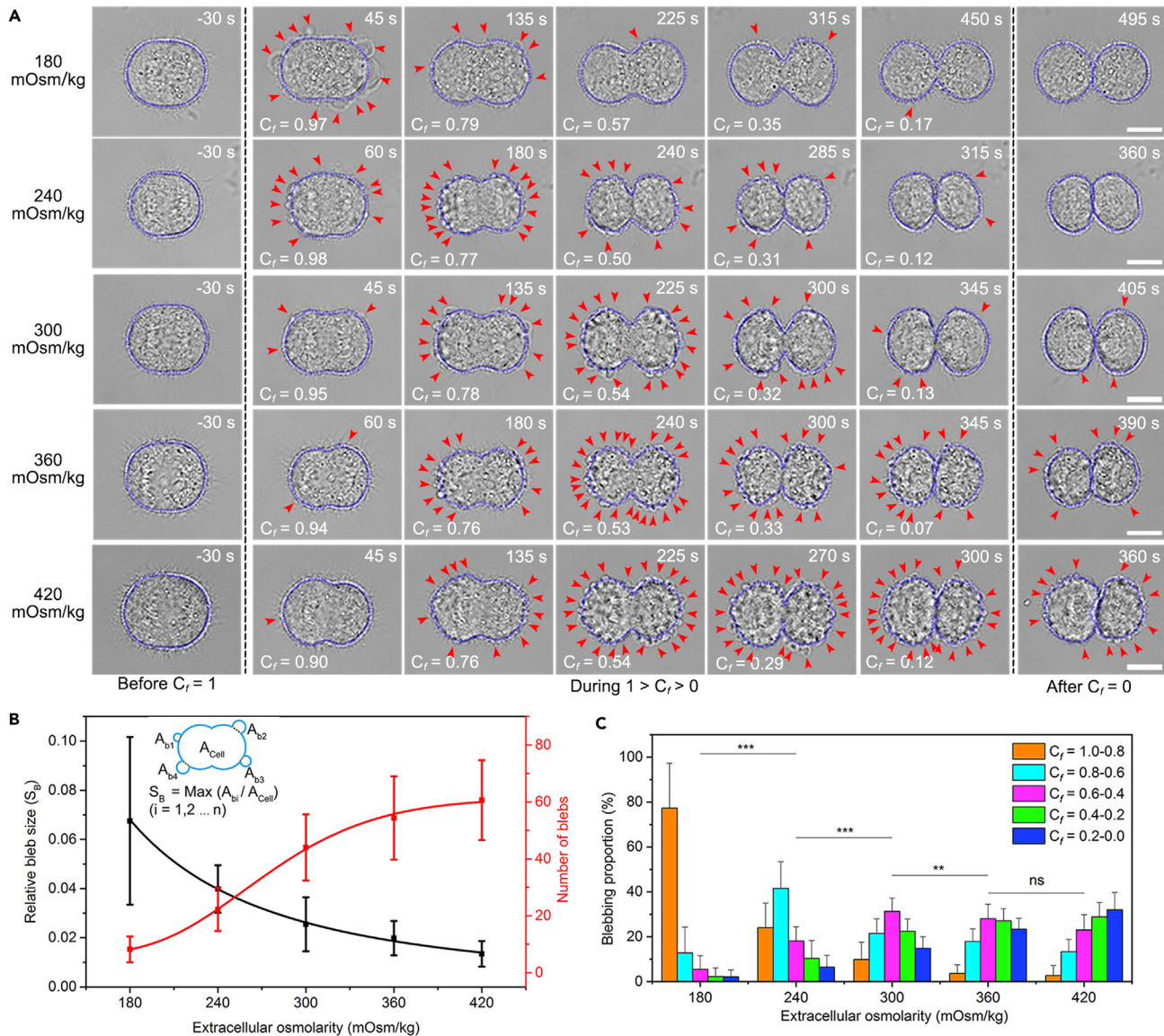


**Figure 2. The effect of the Laplace pressure on the blebbing during cytokinesis**

(A) Snapshots of the cells undergoing cytokinesis in the media with different osmolarities. The numbers in the upper right and lower left of the panels indicate recording time (the moment of solution exchange corresponds to 0 s) and the real-time values of the cytokinesis factor  $C_f$ , respectively. The texts on the bottom point out the ranges of  $C_f$  corresponding to the states of the cells in the panels. The texts on the left sides of the images indicate the osmolarities of the tested media which are introduced at roughly  $C_f = 1$ . The blue dashed lines outline the boundaries of the cells and the red arrowheads point out the blebs on the boundaries. Scale bars, 10  $\mu\text{m}$ .

(B) Effects of the extracellular osmolarity on the relative blebbing size and number ( $n > 30$  cells). The relative blebbing size is the maximum ratio of the projected area of individual bleb to the area of the cell and is explained in the inset. Error bars are SDs.

(C) Blebbing proportions and distributions in the different stages of the cells during cytokinesis in the media with different osmolarities. The osmolarities of the media are indicated below the horizontal axis. ( $n > 50$ , two-way ANOVA followed by Tukey's test). \*\* $P < 0.01$ ; \*\*\* $P < 0.001$ ; ns, not significant. Error bars are SDs.

correspond to the time needed for bleb retraction (Charras et al., 2005). This indicates that the cell blebbing during cytokinesis has already ceased after  $C_f = 0$ .

### The Laplace pressure changes the symmetry of cell division by regulating cell blebbing

We apply a conventional method,  $\phi = \max(A_1, A_2)/\min(A_1, A_2)$ , to investigate the size symmetry of two newborn daughter cells, where  $A_1$  and  $A_2$  are the projected areas of the two daughter cells formed at

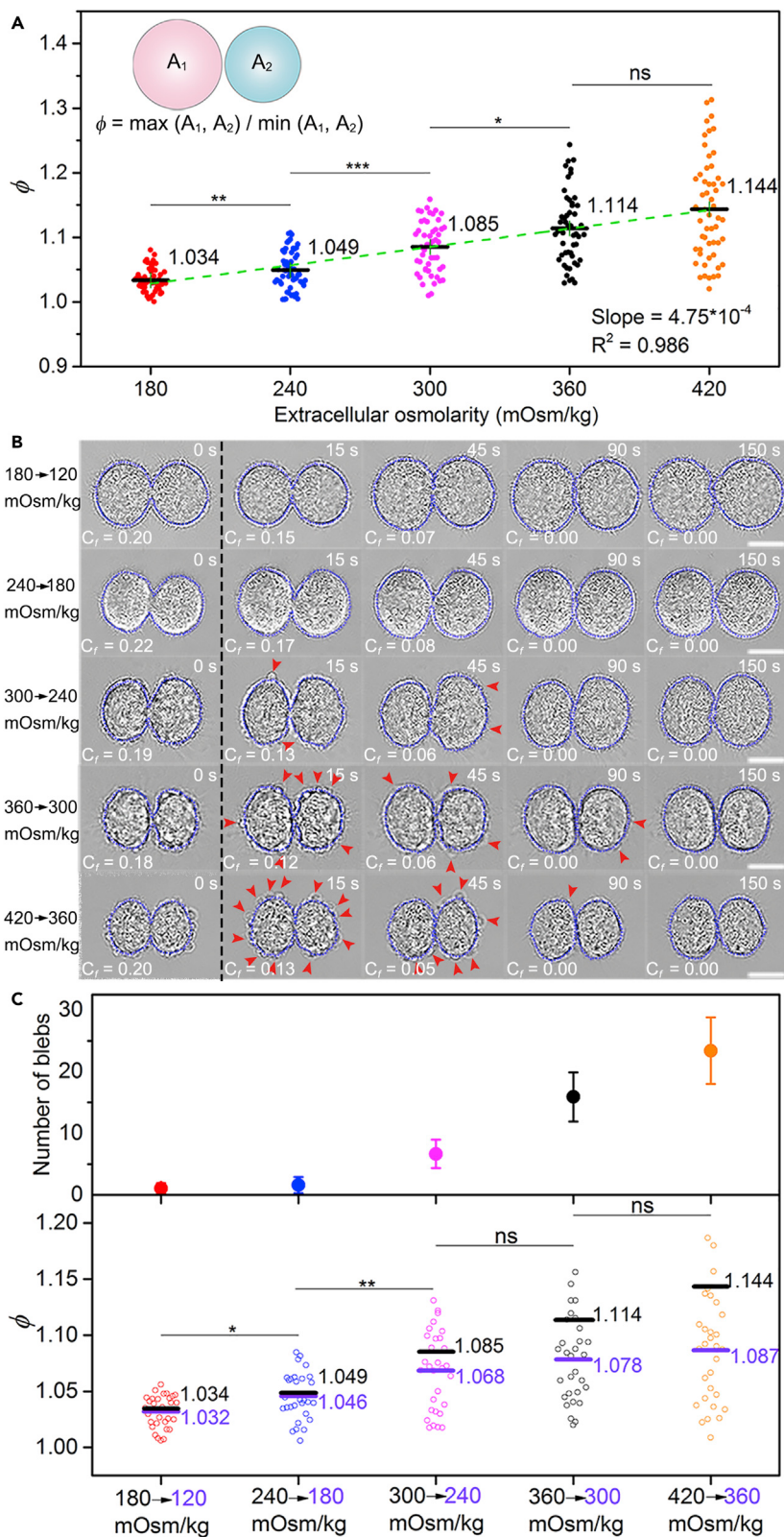


**Figure 3. The effect of the Laplace pressure on the size symmetry of cell division**

(A) Scatterplot of the size symmetry of cell division in the media with different osmolarities. The numbers and the black solid lines in the scatterplot indicate mean values and their positions, respectively. The green dashed line is the fitted line of the mean values, its slope and the coefficient of determination ( $R^2$ ) are shown in the lower right. The inset indicates the definition of the size symmetry of cell division. ( $n > 50$ , Mann-Whitney test). \* $P < 0.05$ ; \*\* $P < 0.01$ ; \*\*\* $P < 0.001$ ; ns, not significant.

(B) Snapshots of the cells undergoing cytokinesis in the media with the osmolarities lower than the superseded ones by 60 mOsm/kg. The solution exchange is performed when the cells just enter into the final stage of cytokinesis ( $C_f \approx 0.2$ ), corresponding to 0 s. The red arrowheads indicate the blebs. Scale bars, 10  $\mu$ m.

(C) Effect of further decreasing extracellular osmolarity on the bleb number retriggered and the symmetry of cell division. Mean values of  $\phi$  for the initial media with osmolarities of 180–420 mOsm/kg (i.e., the results shown in (A)) and the altered media with osmolarities lower than the initial ones by 60 mOsm/kg (120–360 mOsm/kg), are marked as black lines and purple lines, respectively. \* $P < 0.05$ ; \*\* $P < 0.01$ ; ns, not significant ( $n = 30$ , Mann-Whitney test). Error bars are SDs.

$C_f = 0$ , respectively (Kiyomitsu and Cheeseman, 2013; Tan et al., 2015). Obviously, the closer the value of  $\phi$  gets to 1, the better the symmetry of the daughter cells is. In the experiments above, the mean value and the standard deviation of  $\phi$  are computed to be  $\langle \phi \rangle = 1.085$  and  $SD = 0.040$  in the isotonic media, respectively;  $\langle \phi \rangle = 1.034$  ( $SD = 0.019$ ) and  $\langle \phi \rangle = 1.049$  ( $SD = 0.029$ ) in the hypotonic media with 180 and 240 mOsm/kg, respectively; and  $\langle \phi \rangle = 1.114$  ( $SD = 0.055$ ) and  $\langle \phi \rangle = 1.144$  ( $SD = 0.079$ ) in the hypertonic media with 360 and 420 mOsm/kg, respectively (Figure 3A). Thus, these results seem to display that the size symmetry of the daughter cells decreases with the extracellular osmolarity or increases with the Laplace pressure of the mother cell.

The results in Figures 2C and 3A suggest that the cell blebbing and size symmetry of cell division both regulated by the Laplace pressure may be intrinsically connected or the effect of the Laplace pressure on the size symmetry of cell division may be associated with the cell blebbing. To study how the Laplace pressure affects the size symmetry of cell division, we further conduct verification experiments. More specifically, when the tested cells in the media with the different osmolarities evolve into the late stage,  $C_f = 0.2$ –0, we replace the media with the new media again, each with the osmolarity of 60 mOsm/kg lower than superseded one, and see what will happen to the cell blebbing and the size symmetry of cell division. The forming daughter cells are still observed to swell in a geometrically self-similar way within initial 20 s after medium replacement, and then, to continue their unfinished cytokinesis (Figure 3B; Videos S6, S7, S8, S9, and S10). We find that in the media with osmolarities decreasing from 180 to 120 mOsm/kg or from 240 to 180 mOsm/kg, the cell blebbing hardly occurs and the size symmetry of the daughter cells is almost unchanged compared with that in the superseded media; while in the media with osmolarities decreasing, respectively, to 240, 300 and 360 mOsm/kg from 300, 360 and 420 mOsm/kg, quite a few new blebs occur, and almost no blebs remain after  $C_f = 0$ . Our measurements indicate that the mean value of  $\phi$  decreases to  $\langle \phi \rangle = 1.068$  ( $SD = 0.035$ , purple line) from  $\langle \phi \rangle = 1.085$  (black line), to  $\langle \phi \rangle = 1.078$  ( $SD = 0.037$ ) from  $\langle \phi \rangle = 1.114$ , and to  $\langle \phi \rangle = 1.087$  ( $SD = 0.048$ ) from  $\langle \phi \rangle = 1.144$ , respectively (Figure 3C). Therefore, for the cells evolving into the late stage in the hypotonic media, decreasing the extracellular osmolarity does not cause the cells to regenerate blebs nor increases the size symmetry of the daughter cells, whereas for the isotonic and hypertonic media, the opposite is true. This is an indication that only when the Laplace pressure can trigger cell blebs, can the symmetry of cell division be enhanced, thus highlighting the essential role of cell blebbing in ensuring symmetric cell division, and suggesting that the Laplace pressure changes the symmetry of cell division by regulating cell blebbing.

In addition, when the cells in the media with the different osmolarities evolve close to  $C_f = 0$  again in the experiments here, we replace the media to enhance the Laplace pressures of the cells again. The results show that once the blebbing of a cell undergoing cytokinesis already completes, the blebbing does not occur even if increasing the Laplace pressure again (Figure S2). This result means that the blebbing number of a cell undergoing cytokinesis is limited. Together with the results in Figure 2C, it indicates that the increment of the Laplace pressure accelerates the completion of blebbing activity during cytokinesis. In other words, the higher the Laplace pressure is, the greater the proportion of the blebbing in the earlier stage is, the sooner the blebbing activity completes.

**Cell blebbing enhances the symmetry of cell division**

To understand the biological significances of cell blebbing during mitosis, we apply Concanavalin A (Con A) to treat the cells at  $C_f = 1$ , which is a tetravalent lectin and can sufficiently inhibit cell blebbing during

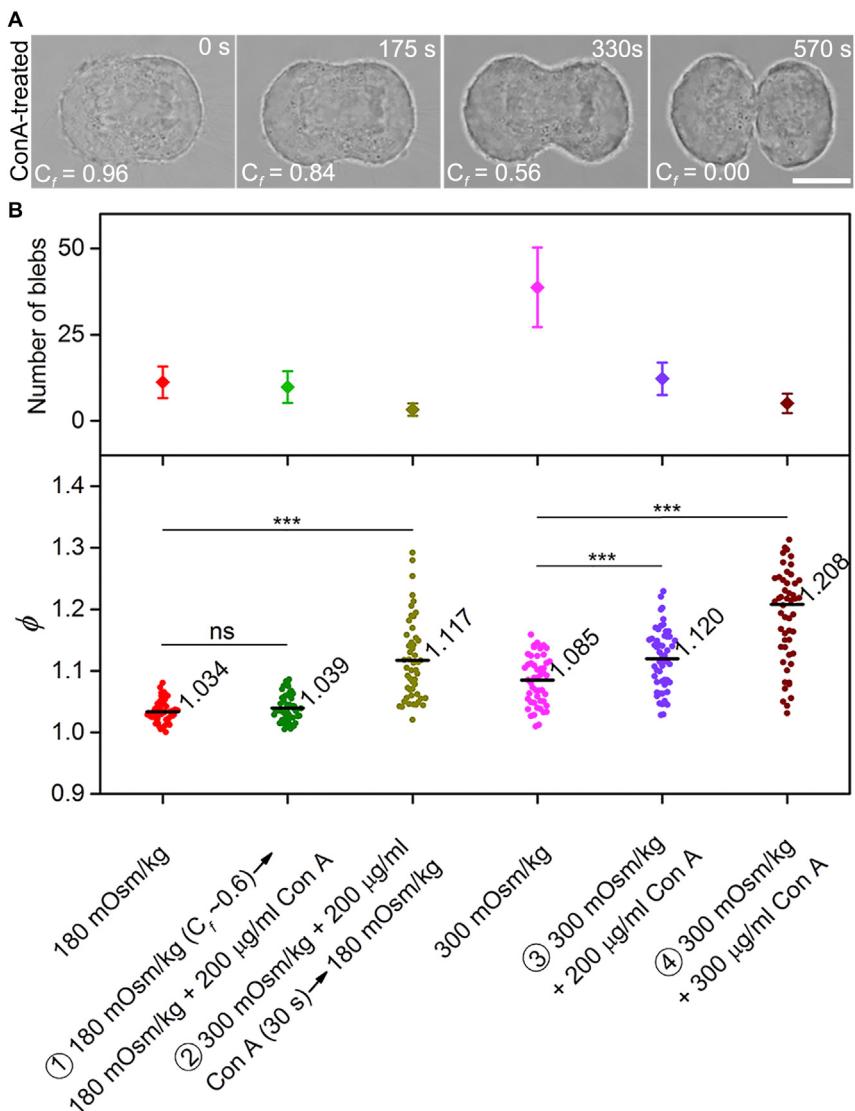


**Figure 4. Inhibiting blebbing decreases the symmetry of cell division**

(A) Snapshots of the evolution of a cell undergoing cytokinesis in the isotonic medium with Con A of 200  $\mu\text{g}/\text{mL}$ . Cell blebbing decreases significantly relative to that in the absence of Con A (A) Scale bar, 10  $\mu\text{m}$ .

(B) Effect of Con A on the bleb number and the size symmetry of cell division. Case ①: The cells undergoing cytokinesis in hypotonic medium (180 mOsm/kg) are treated with Con A of 200  $\mu\text{g}/\text{mL}$  after the cell blebbing activities mainly finish ( $C_f \approx 0.6$ ); Case ②: The cells are treated in isotonic medium (300 mOsm/kg) with Con A of 200  $\mu\text{g}/\text{mL}$  for 30 s when they are about to enter into cytokinesis. Immunofluorescence image indicates that the Con A of 200  $\mu\text{g}/\text{mL}$  can effectively bind to cell within 30 s, manifested as the roughly unchanged fluorescence intensity of Con A with time after 30 s (Figure S3). Then the isotonic medium is replaced by a hypotonic solution with osmolarity of 180 mOsm/kg; Case ③: The cells undergoing cytokinesis are treated in isotonic medium (300 mOsm/kg) with Con A of 200  $\mu\text{g}/\text{mL}$ ; Case ④: The cells undergoing cytokinesis are treated in isotonic medium (300 mOsm/kg) with Con A of 300  $\mu\text{g}/\text{mL}$ . \*\*\*P < 0.001; ns, not significant. Error bars are SDs.

cytokinesis by binding to cell surface glycoproteins and acting to cross-link the cell cortex effectively (Rose-nblatt et al., 2004; Sedzinski et al., 2011). When the normal cultured media are separately replaced by the same osmolarity media with Con A of 200 and 300  $\mu\text{g}/\text{mL}$ , the bleb numbers decrease separately by roughly 68% and 86%, and correspondingly, the mean values of  $\phi$  change to  $\langle\phi\rangle = 1.120$  ( $\text{SD} = 0.050$ ,  $n = 53$ ) and  $\langle\phi\rangle = 1.208$  ( $\text{SD} = 0.093$ ,  $n = 58$ ) from the original mean value  $\langle\phi\rangle = 1.085$ , respectively (Figure 4A, Cases ③ and ④ in Figure 4B). The results here indicate that inhibiting cell blebbing during cytokinesis effectively decreases the size symmetry of cell division.

In particular, when we treat the cells with Con A of 200  $\mu\text{g/mL}$  in isotonic medium (300 mOsm/kg) for 30 s before introducing hypotonic medium with 180 mOsm/kg, the bleb numbers of the tested cells decreased by about 70% ( $n = 51$ ) compared with that for the case where the medium is directly replaced by the hypotonic medium with 180 mOsm/kg and the mean value of  $\phi$  increases significantly to  $\langle \phi \rangle = 1.117$  ( $SD = 0.066$ ) from the original mean value  $\langle \phi \rangle = 1.034$  (Case ② in Figure 4B). This result demonstrates that the cell blebbing driven by the Laplace pressure is dominant in affecting the size symmetry of cell division in contrast to changing extracellular osmolarity. So, the sufficiency of the cell blebbing during cytokinesis is directly responsible for regulating the size symmetry of cell division. Note that treating cells with Con A can lead to increased cell stiffness and decreased deformability (Chaigne et al., 2013), which possibly break the symmetry of cell division. This raises the question that which is the true contributor to the division symmetry. To answer this question, we carry out a supplementary experiment, in which the tested cells are initially incubated in the hypotonic medium with 180 mOsm/kg, the addition of Con A to cells is implemented after the blebbing activities basically complete in the stage of  $C_f \approx 0.6\text{--}0.8$ . We find the division symmetry of the Con A-treated cells being almost unchanged (Case ① in Figure 4B), suggesting that it is the cell blebbing that accounts for the effect of symmetric cell division. In addition, we perform another experiment, in which the cells undergoing cytokinesis in different media (180, 240, 300, 360, and 420 mOsm/kg) with Con A of 300 mg/mL. In these cases, the cell blebbing hardly occurs during cytokinesis, and the mean values of  $\phi$  for different groups remain approximately the same, which are about 1.2. This result further highlights the significance of cell blebbing in ensuring symmetric cell division.

### Change to the Laplace pressure makes the structural change of cell boundary

In order to explore the effects of the Laplace pressures generated in the tested media with different osmolarities on cell structures, by labeling actin with FITC-phalloidin, we observe the cortex-membrane boundary of the cells evolving close to  $C_f = 0$  in the tested media. We find that there are some defects remaining within the daughter cell boundaries in the hypertonic media at the end of cytokinesis. Here, these defects are reflected as actin deficiency or aggregation in the cortex, as clearly observed in immunofluorescence images, and correspond to detachment of the plasma membrane from the cell cortex caused by cortex ruptures or missing linker proteins. However, in the hypotonic media there is hardly any defect within the two newborn daughter cell boundaries. The fluorescence-intensity distribution analysis also indicates that increasing the Laplace pressure facilitates the uniformity of the cortex distribution in the cortex-membrane boundary of the two daughter cells (Figure 5). We further perform live cell imaging experiments showing that the occurrence of bleb changes the actin distribution of the two daughter cells (Figure S4). In fact, the boundary defects are formed in the course of cell rounding immediately prior to cytokinesis (Cadart et al., 2014; Gauthier et al., 2012). On the one hand, cell blebbing is a pressure-driven membrane protrusion and occurs at the position of boundary defect (Paluch and Raz, 2013; Strychalski and Guy, 2016). On the other hand, the defect can be repaired by the blebbing retraction due to the reassembly of cortex during blebbing (Charras and Paluch, 2008; Charras et al., 2006) (Figure S5). Therefore, the high Laplace pressure generated in the hypotonic media adequately drives the accomplishment of the cell blebbing during cytokinesis and effectively repairs the boundary defects. On the contrary, the low Laplace pressure generated in the hypertonic media does not adequately accomplish the cell blebbing so that some defects still remain within the formed daughter cell boundaries. The results here mean that change to the Laplace pressure of a cell during cytokinesis varies the structure of the cortex by virtue of pressure-driven cell blebbing.

### Uniformity of cell boundary determines the symmetry of cell division

We employ a local delivery setup to create a localized diffusion gradient field of Cytochalasin B (CB) from one pole of a tested cell to the other (Figure 6A). Because the CB acts to inhibit actin polymerization (MacLean-Fletcher and Pollard, 1980), this gradient field can not only produce the boundary defects but also prevent the original defects from being repaired by blebbing retraction, thus causing more boundary damages in the pole closer to the CB source. In addition, CB treatment should also negatively affect the intracellular pressure and the Laplace pressure by disrupting actomyosin contractility, which is detrimental to the sufficiency of cell blebbing and the repair of the defects in the cortex, as well as the boundary uniformity. We find that the boundary uniformity, which is affected by the imbalance distribution of the boundary defects between the two cell poles (Figure S6), finally results in asymmetric cell division with a bigger daughter cell closer to the CB source (Figure 6B).

However, when we replace the isotonic medium by the same osmolarity medium with CB of 0.05  $\mu\text{M}$  to ensure the two poles of the tested cells having the same environment, i.e. to ensure the daughter cell

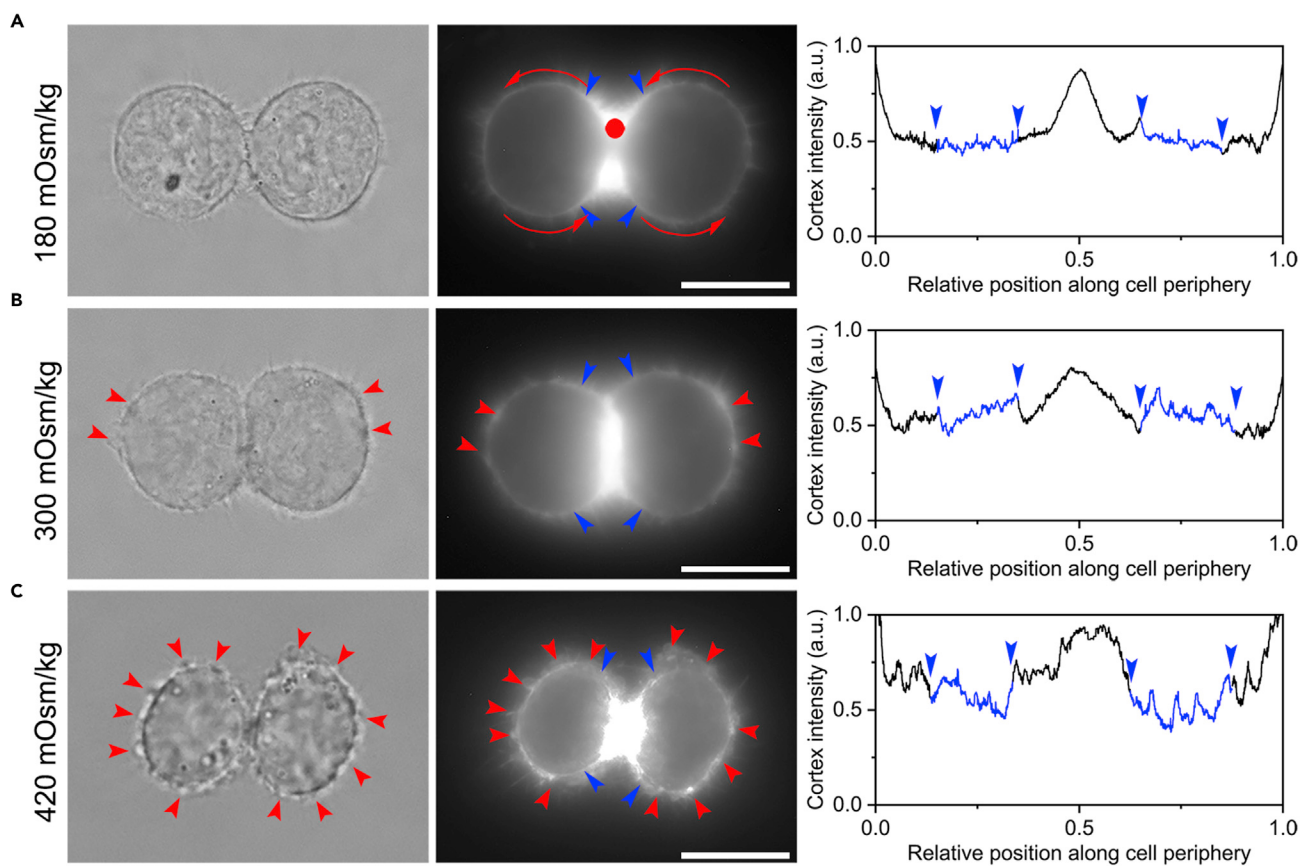


**Figure 5. The Laplace pressure changes the cortex structure**

(A–C) Experimental results showing the cortex of the cells in media with the osmolarities of (A) 180, (B) 300, and (C) 420 mOsm/kg when the cytokinesis mainly finishes. The red arrowheads indicate the blebs. The Figures are arranged in three columns, from left to right: (i) bright field images of the representative cells at the end of cytokinesis; (ii) immunofluorescence images of actin. Actin is labeled with FITC-phalloidin after fixation with paraformaldehyde and immunofluorescence images are projections of Z stacks of 20 mid-section slices that cover a total depth of 7.32  $\mu\text{m}$ ; (iii) cortical distribution measured counterclockwise from the central furrow (red dot), the blue parts in the curves correspond to the positions indicated by blue arrow heads in (ii), a.u., arbitrary units. Scale bars, 10  $\mu\text{m}$ .

boundaries formed at these poles producing the same defects statistically, we find that it leads to a relatively symmetric cell division compared with the results of local cytochalasin delivery experiment. However, the formed daughter cells slightly increase in size compared with normal division (Figure 6C). This result displays that the uniformity of cell boundary effectively determines the symmetry of cell division and the defects induce softening of the cortex. In addition, we perform a live cell imaging experiment in which the microtubule marker mCherry- $\alpha$ -tubulin is used to label the mitotic spindle for the Con A treatment ( $n = 10$ ) and local CB delivery ( $n = 10$ ) experiments. As shown in Figure S7, the spindle displays no obvious instability in response to the treatment of Con A and CB during cytokinesis.

Further, by applying the Young-Laplace equation and damage mechanics, we build a cell shape change model during cytokinesis to demonstrate that the uniformity of cell boundary determines the symmetry of cell division. The shape of a cell during cytokinesis can be geometrically assumed as two connected spherical caps (Yoneda and Dan, 1972) (Figure 6D), its cortex-membrane boundary is deemed to be an elastic material and the defects within the boundary are considered as the damages of the material. So, the elastic equations of the cell are written by (Boal, 2012; Lemaitre, 1996)

$$\tau_i = (1 - f_i)K_0\varepsilon_i \quad (i = 1, 2) \quad (\text{Equation 1})$$

where  $\tau_i$  ( $i = 1, 2$ ) are the surface tensions of the cortex-membrane boundaries of the two forming daughter cells at two poles of the cell; the subscripts,  $i = 1, 2$ , separately correspond to the two daughter cells;  $K_0$  is

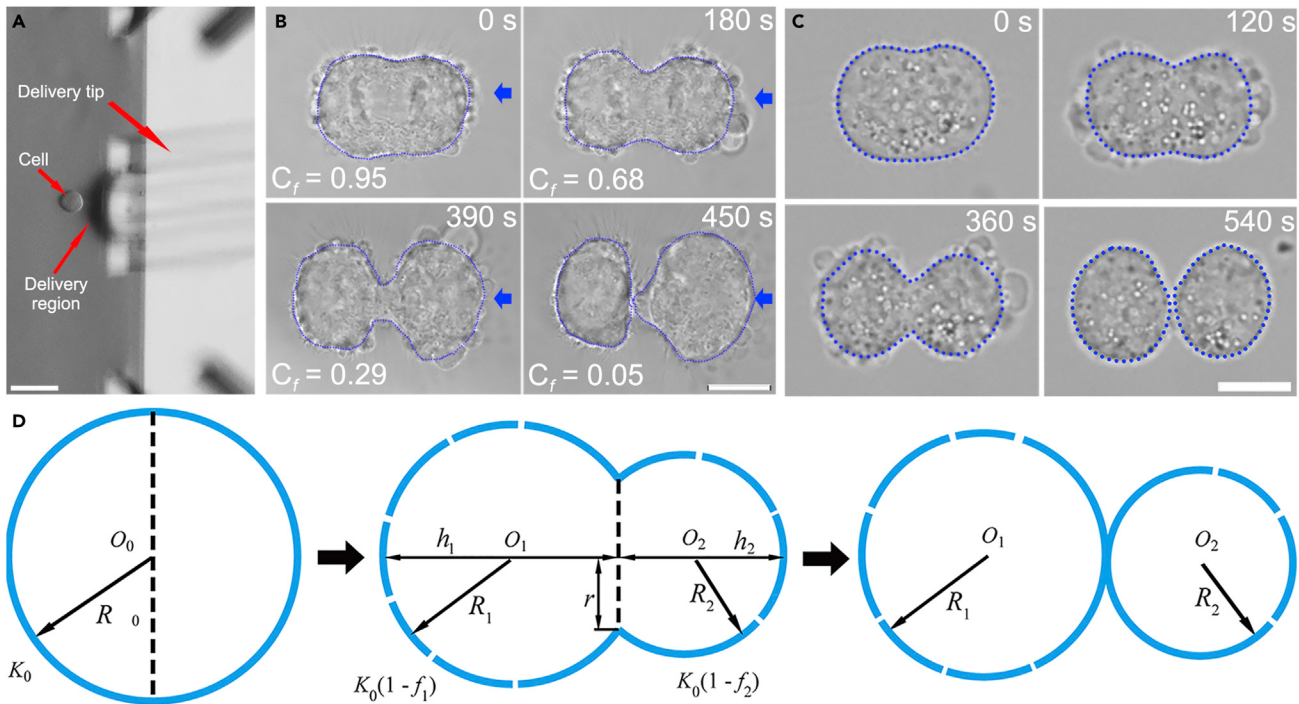


**Figure 6. Uniformity of Cell Boundary Determines the Symmetry of Cell Division**

(A) The local delivery experiment. The red arrows point out the positions of tested cell, delivery region and the tip of local delivery setup, respectively, where the delivery region is displayed by trypan blue solution. Scale bar, 20 μm.

(B) Snapshots of a dividing cell under the effect of localized Cytochalasin B. The numbers in the upper right and lower left of the panels indicate recording time (0 s is the onset of drug delivery) and the real-time values of the cytokinesis factor  $C_f$ , respectively. Blue arrows indicate the cell pole that is immersed in the delivery region. The blue dashed lines outline the boundaries of the cell. Scale bar, 10 μm.

(C) Snapshots of a dividing cell immersed in the solution with low dose of Cytochalasin B ( $0.05 \mu\text{M}$ ).

(D) Illustration of a dividing cell with unbalanced boundary defects characterized by the damage factor  $f_i$  ( $i = 1, 2$ ). The shape of the cell during cytokinesis is geometrically described as two connected spherical caps, where  $R_i$ ,  $h_i$ ,  $f_i$  ( $i = 1, 2$ ) and  $r$  change with the cytokinesis process of the cell.

the initial boundary elastic modulus at the state that the cleavage furrow of the cell just emerged, and it is deemed that the same amount of defects are included in the forming daughter cell boundaries of the two sides of the cleavage furrow;  $f_i$  ( $i = 1, 2$ ) stand for the evolving damage factors of the two forming daughter cell boundary, respectively, which usually satisfy  $0 < f_i < 1$ , but satisfy  $f_i = 0$  at the initial state that the cleavage furrow just emerges. Obviously, as  $f_1 = f_2$ , the two forming daughter cell boundaries are uniform, while  $f_1 \neq f_2$ , the daughter cell boundaries are not uniform;  $\varepsilon_i$  ( $i = 1, 2$ ) are separately the areal strains of the daughter cells, and are written by

$$\varepsilon_i = \frac{\pi(r^2 + h_i^2) - 2\pi R_0^2}{2\pi R_0^2} = \frac{1}{2} \frac{r^2 + h_i^2}{R_0^2} - 1 \quad (i = 1, 2) \quad (\text{Equation 2})$$

where  $R_0$  is the initial radius of the cell;  $r$  is the radius of the contractile ring;  $R_i$  and  $h_i$  ( $i = 1, 2$ ) are the radii and heights of the two forming daughter cells, respectively. All the parameters including  $\tau_i$ ,  $\varepsilon_i$ ,  $r$ ,  $R_i$  and  $h_i$  are functions of time. Geometrically,  $h_i$  develops from the emergence of the cleavage furrow,  $h_i = R_0$  to the accomplishment of the contractile-ring contraction,  $h_i = 2R_i$ . They geometrically satisfy

$$r^2 = R_i^2 - (R_i - h_i)^2 \quad (i = 1, 2) \quad (\text{Equation 3})$$

The Young-Laplace equation for each daughter cell is expressed as

$$\Delta p = \frac{2\tau_i}{R_i} \quad (i = 1, 2) \quad (\text{Equation 4})$$

where  $\Delta p$  stands for the Young-Laplace pressure of the two forming daughter cells at the timely state.

Substituting (Equations 1–3) into (Equation 4) yields

$$\frac{f(h_1)}{f(h_2)} = \frac{1 - f_2}{1 - f_1} \quad (\text{Equation 5})$$

where

$$f(h_i) = \frac{2h_i}{r^2 + h_i^2} \left( \frac{1}{2} \frac{r^2 + h_i^2}{R_0^2} - 1 \right) \quad (i = 1, 2) \quad (\text{Equation 6})$$

Noting the fact that geometrically  $h_i \geq r$ , we readily demonstrate that  $f(h_i)$  is a monotonically increasing function with respect to  $h_i$  by using  $d f(h_i)/dh_i \geq 0$ . According to (Equations 5 and 3), we obtain the results that if  $f_1 = f_2$ , i.e. the two forming daughter cell boundaries are uniform, then  $h_1 = h_2$  and  $R_1 = R_2$ , i.e. the cell division is symmetric; and if  $f_1 > f_2$ , i.e. the two forming daughter cell boundaries are not uniform, then  $h_1 > h_2$  and  $R_1 > R_2$ , i.e. the cell division is asymmetric and the daughter cell with a greater extent defect is larger in size. So, here we prove that the uniformity of cell boundary determines the symmetry of cell division.

## Conclusions

In the present work, by virtue of regulating extracellular osmolarity, we detailedly investigate the effects of the Laplace pressure on the changes of cell morphology during cytokinesis. First of all, we find that the Laplace pressure can directly control the distribution and size of cell blebbing during cytokinesis: the larger the Laplace pressure of a cell during cytokinesis is, the sooner the blebbing activity completes, at the same time, the fewer the mean number of blebs is and the larger the mean size of blebs is.

Further, we demonstrate that the variation of the Laplace pressure of a cell during cytokinesis cannot directly change the symmetry of cell division, but by virtue of changing the cell blebbing during cytokinesis it can adjust the symmetry. Indirectly, the larger the Laplace pressure is, the more symmetric the newborn daughter cells are.

Finally, we give the mechanism that the Laplace pressure adjusts the symmetry of cell division by virtue of changing the cell blebbing during cytokinesis: the cell boundary uniformity at the two sides of the cell furrow during cytokinesis determines the size symmetry of the two daughter cells.

Traditionally, the main mechanism controlling the symmetry of cell division is that the mitotic spindle directs the assembly and contraction of the contractile ring and guides the formation of a single central furrow (McNally, 2013; Morin and Bellaïche, 2011), wherein both central positioning and proper orientation of the spindle play a key role (Siller and Doe, 2009). In this course, the polar cortex contractility destabilizes the position of the cytokinetic furrow and makes the shape of the symmetrically dividing cell inherently unstable (Connell et al., 2011; Ou et al., 2010; Sedzinski et al., 2011). The competition between contraction dynamics and cortex turnover is responsible for the cytoplasmic flow and unstable cell shape (Sedzinski et al., 2011). The mechanism presented here is that the Laplace pressure of a cell during cytokinesis changes the boundary structure of the cell by changing the blebbing characteristics in order to realize adjusting the symmetry of cell division. In fact, these mechanisms are not mutually exclusive but instead are closely interrelated. On the one hand, the spindle positioning and orientation rely on the pulling forces of microtubule motors such as dynein anchored to the cell cortex (Grill et al., 2003, 2005). The Laplace pressure-regulated intactness of cortex on both sides of the dividing cells favors the balance of number of these force generators, which in turn influences the spindle positioning and orientation, and the symmetry of cell division. On the other hand, the developed mechanically symmetric cell cortex contributes to generating more balanced polar contractile forces, which can stabilize cell shape and favor symmetric cell division.

It is noteworthy that membrane blebs, primarily viewed as a by-product of cytokinesis, are proposed to act as valves releasing cortical contractility to stabilize cell shape (Charras, 2008; Sedzinski et al., 2011). Here, our results uncover the essential role of blebs in regulating the uniformity of cell boundary and symmetric cell division. In all the experiments above, the existing spindle mechanisms regulating the symmetric cell division are persistently in effect; however, just varying the Laplace pressures of the tested cells to make the change of the blebbing during cytokinesis can still effectively affect the symmetry of cell division to the directions that the changes of the pressures expect. Accordingly, the Laplace pressure of a cell during cytokinesis may play a more fundamental role in regulating the size symmetry of cell division.

Taken together, these results presented here provide further insights into the role of Laplace pressure in ensuring symmetric cell division and highlight the significance of pressure-driven blebbing, which is endowed with new functions. Moreover, the fact that Laplace pressure can modify the cell boundary structure to regulate cell division implies that the pressure may play much more fundamental roles in other cell boundary-dependent cellular processes, such as cell spreading and migration, cancer metastasis, intercellular signal transduction, and further studies are needed.

### Limitations of the study

In the present work, we show how the Laplace pressure affects the cell blebbing, division symmetry, as well as structural change of cell boundary for cells undergoing symmetric cell division. It needs to be explored further whether these underlying mechanisms elucidated here also apply to the case of asymmetric cell division. In addition, the dependence of cytokinesis speed and daughter cell fate on the Laplace pressure for both symmetric and asymmetric cell division remains to be determined.

### STAR★METHODS

Detailed methods are provided in the online version of this paper and include the following:

- KEY RESOURCES TABLE
- RESOURCE AVAILABILITY
  - Lead contact
  - Materials availability
  - Data and code availability
- EXPERIMENTAL MODEL AND SUBJECT DETAILS
  - Cell lines
- METHOD DETAILS
  - Solution exchange assay
  - Local cytochalasin B delivery
  - Cell labeling and imaging
  - Cell volume calculation
  - Laplace pressure calculation
  - $C_f$  calculation, bleb size and counting
- QUANTIFICATION AND STATISTICAL ANALYSIS

### SUPPLEMENTAL INFORMATION

Supplemental information can be found online at <https://doi.org/10.1016/j.isci.2021.102945>.

### ACKNOWLEDGMENTS

We thank Dr. Wei Li in North China Institute of Aerospace Engineering for mathematic advices. This work has been supported by the National Natural Science Foundation of China (Grant Nos. 11972041 and 11902327), Youth Innovation Promotion Association CAS, the Strategic Priority Research Program of the Chinese Academy of Sciences (Grant No. XDB22040102).

### AUTHOR CONTRIBUTIONS

F.S. suggested this study, analyzed data, and wrote the paper; X.H.W. designed and performed all the experiments, analyzed data, and wrote the paper; L.L. performed the theoretical analysis, analyzed data, and wrote the paper; Y.F.S. and J.C.W. analyzed data. All authors discussed the results and commented on the manuscript.

### DECLARATION OF INTERESTS

The authors declare that they have no competing interests.

Received: December 31, 2020

Revised: April 28, 2021

Accepted: July 29, 2021

Published: September 24, 2021

## REFERENCES

- Alert, R., and Casademunt, J. (2016). Bleb nucleation through membrane peeling. *Phys. Rev. Lett.* 116, 068101.
- Boal, D. (2012). *Mechanics of the Cell* (Cambridge University Press).
- Boucrot, E., and Kirchhausen, T. (2007). Endosomal recycling controls plasma membrane area during mitosis. *Proc. Natl. Acad. Sci. U.S.A.* 104, 7939–7944.
- Burton, K., and Taylor, D.L. (1997). Traction forces of cytokinesis measured with optically modified elastic substrata. *Nature* 385, 450–454.
- Butt, H., Graf, K., and Kappl, M. (2013). *Physics and Chemistry of Interfaces* (Wiley-VCH Verlag GmbH).
- Cadart, C., Zlotek-Zlotkiewicz, E., Le Berre, M., Piel, M., and Matthews, H.K. (2014). Exploring the function of cell shape and size during mitosis. *Dev. Cell* 29, 159–169.
- Cayley, S., and Record, M.T., Jr. (2003). Roles of cytoplasmic osmolytes, water, and crowding in the response of Escherichia coli to osmotic stress: biophysical basis of osmoprotection by glycine betaine. *Biochemistry* 42, 12596–12609.
- Chaigne, A., Campillo, C., Gov, N.S., Voituriez, R., Azoury, J., Umaña-Díaz, C., Almonacid, M., Queguiner, I., Nassoy, P., Sykes, C., et al. (2013). A soft cortex is essential for asymmetric spindle positioning in mouse oocytes. *Nat. Cell Biol.* 15, 958–966.
- Charras, G., and Paluch, E. (2008). Blebs lead the way: how to migrate without lamellipodia. *Nat. Rev. Mol. Cell Biol.* 9, 730–736.
- Charras, G.T. (2008). A short history of blebbing. *J. Microsc.* 231, 466–478.
- Charras, G.T., Coughlin, M., Mitchison, T.J., and Mahadevan, L. (2008). Life and times of a cellular bleb. *Biophys. J.* 94, 1836–1853.
- Charras, G.T., Hu, C.K., Coughlin, M., and Mitchison, T.J. (2006). Reassembly of contractile actin cortex in cell blebs. *J. Cell Biol.* 175, 477–490.
- Charras, G.T., Yarrow, J.C., Horton, M.A., Mahadevan, L., and Mitchison, T.J. (2005). Non-equilibration of hydrostatic pressure in blebbing cells. *Nature* 435, 365–369.
- Chengappa, P., Sao, K., Jones, T.M., and Petrie, R.J. (2018). Intracellular pressure: a driver of cell morphology and movement. *Int. Rev. Cell Mol. Biol.* 337, 185–211.
- Connell, M., Cabernard, C., Ricketson, D., Doe, C.Q., and Prehoda, K.E. (2011). Asymmetric cortical extension shifts cleavage furrow position in Drosophila neuroblasts. *Mol. Biol. Cell* 22, 4220–4226.
- Dorn, J.F., and Maddox, A.S. (2011). Cytokinesis: cells go back and forth about division. *Curr. Biol.* 21, R848–R850.
- Erickson, C.A., and Trinkaus, J.P. (1976). Microvilli and blebs as sources of reserve surface membrane during cell spreading. *Exp. Cell Res.* 99, 375–384.
- Fishkind, D.J., Cao, L.G., and Wang, Y.L. (1991). Microinjection of the catalytic fragment of myosin light chain kinase into dividing cells: effects on mitosis and cytokinesis. *J. Cell Biol.* 114, 967–975.
- Gauthier, N.C., Masters, T.A., and Sheetz, M.P. (2012). Mechanical feedback between membrane tension and dynamics. *Trends Cell Biol.* 22, 527–535.
- Grill, S.W., Howard, J., Schäffer, E., Stelzer, E.H., and Hyman, A.A. (2003). The distribution of active force generators controls mitotic spindle position. *Science* 301, 518–521.
- Grill, S.W., Kruse, K., and Jülicher, F. (2005). Theory of mitotic spindle oscillations. *Phys. Rev. Lett.* 94, 108104.
- Guan, Y.Y., Wang, G.L., and Zhou, J.G. (2006). The CIC-3 Cl<sup>-</sup> channel in cell volume regulation, proliferation and apoptosis in vascular smooth muscle cells. *Trends Pharmacol. Sci.* 27, 290–296.
- Kim, N.S., and Lee, G.M. (2002). Response of recombinant Chinese hamster ovary cells to hyperosmotic pressure: effect of Bcl-2 overexpression. *J. Biotechnol.* 95, 237–248.
- Kiyomitsu, T. (2015). Mechanisms of daughter cell-size control during cell division. *Trends Cell Biol.* 25, 286–295.
- Kiyomitsu, T., and Cheeseman, I.M. (2013). Cortical dynein and asymmetric membrane elongation coordinately position the spindle in anaphase. *Cell* 154, 391–402.
- Lang, F., Föller, M., Lang, K.S., Lang, P.A., Ritter, M., Gulbins, E., Vereninov, A., and Huber, S.M. (2005). Ion channels in cell proliferation and apoptotic cell death. *J. Membr. Biol.* 205, 147–157.
- Le Bihan, D., Urayama, S., Aso, T., Hanakawa, T., and Fukuyama, H. (2006). Direct and fast detection of neuronal activation in the human brain with diffusion MRI. *Proc. Natl. Acad. Sci. U.S.A.* 103, 8263–8268.
- Lemaître, J. (1996). *A Course on Damage Mechanics* (Springer-Verlag).
- Li, L., Hu, J., Różycki, B., and Song, F. (2020). Intercellular receptor-ligand binding and thermal fluctuations facilitate receptor aggregation in adhering membranes. *Nano Lett.* 20, 722–728.
- MacLean-Fletcher, S., and Pollard, T.D. (1980). Mechanism of action of cytochalasin B on actin. *Cell* 20, 329–341.
- McNally, F.J. (2013). Mechanisms of spindle positioning. *J. Cell Biol.* 200, 131–140.
- Morin, X., and Bellaïche, Y. (2011). Mitotic spindle orientation in asymmetric and symmetric cell divisions during animal development. *Dev. Cell* 21, 102–119.
- Ohtsubo, M., and Hiramoto, Y. (1985). Regional difference in mechanical properties of the cell surface in dividing echinoderm eggs. *Develop. Growth Differ.* 27, 371–383.
- Oldenhof, H., Blässe, A.K., Wolkers, W.F., Bollwein, H., and Sieme, H. (2011). Osmotic properties of stallion sperm subpopulations determined by simultaneous assessment of cell volume and viability. *Theriogenology* 76, 386–391.
- Ou, G., Stuurman, N., D'Ambrosio, M., and Vale, R.D. (2010). Polarized myosin produces unequal-size daughters during asymmetric cell division. *Science* 330, 677–680.
- Paluch, E.K., and Raz, E. (2013). The role and regulation of blebs in cell migration. *Curr. Opin. Cell Biol.* 25, 582–590.
- Petrie, R.J., and Koo, H. (2014). Direct measurement of intracellular pressure. *Curr. Protoc. Cell Biol.* 63, 12.9.1–12.9.9.
- Reichl, E.M., Effler, J.C., and Robinson, D.N. (2005). The stress and strain of cytokinesis. *Trends Cell Biol.* 15, 200–206.
- Rosenblatt, J., Cramer, L.P., Baum, B., and McGee, K.M. (2004). Myosin II-dependent cortical movement is required for centrosome separation and positioning during mitotic spindle assembly. *Cell* 117, 361–372.
- Sansregret, L., and Petronczki, M. (2013). Born equal: dual safeguards for daughter cell size symmetry. *Cell* 154, 269–271.
- Sao, K., Jones, T.M., Doyle, A.D., Maity, D., Schevitz, G., Chen, Y., Gunning, P.W., and Petrie, R.J. (2019). Myosin II governs intracellular pressure and traction by distinct tropomyosin-dependent mechanisms. *Mol. Biol. Cell* 30, 1170–1181.
- Sedzinski, J., Biro, M., Oswald, A., Tinevez, J.Y., Salbreux, G., and Paluch, E. (2011). Polar actomyosin contractility destabilizes the position of the cytokinetic furrow. *Nature* 476, 462–466.
- Siller, K.H., and Doe, C.Q. (2009). Spindle orientation during asymmetric cell division. *Nat. Cell Biol.* 11, 365–374.
- Sorce, B., Escobedo, C., Toyoda, Y., Stewart, M.P., Cattin, C.J., Newton, R., Banerjee, I., Stettler, A., Roska, B., Eaton, S., et al. (2015). Mitotic cells contract actomyosin cortex and generate pressure to round against or escape epithelial confinement. *Nat. Commun.* 6, 8872.
- Stewart, M.P., Helenius, J., Toyoda, Y., Ramanathan, S.P., Muller, D.J., and Hyman, A.A. (2011). Hydrostatic pressure and the actomyosin cortex drive mitotic cell rounding. *Nature* 469, 226–230.
- Strychalski, W., and Guy, R.D. (2016). Intracellular pressure dynamics in blebbing cells. *Biophys. J.* 110, 1168–1179.
- Tan, C.H., Gasic, I., Huber-Reggi, S.P., Dudka, D., Barisic, M., Maiato, H., and Meraldi, P. (2015). The equatorial position of the metaphase plate ensures symmetric cell divisions. *Elife* 4, e05124.

Tinevez, J.Y., Schulze, U., Salbreux, G., Roensch, J., Joanny, J.F., and Paluch, E. (2009). Role of cortical tension in bleb growth. *Proc. Natl. Acad. Sci. USA* 106, 18581–18586.

Wehner, F., Olsen, H., Tinel, H., Kinne-Saffran, E., and Kinne, R.K. (2003). Cell volume regulation: osmolytes, osmolyte transport, and signal

transduction. *Rev. Physiol. Biochem. Pharmacol.* 148, 1–80.

Yanai, M., Kenyon, C.M., Butler, J.P., Macklem, P.T., and Kelly, S.M. (1996). Intracellular pressure is a motive force for cell motion in Amoeba proteus. *Cell Motil. Cytoskel.* 33, 22–29.

Yoneda, M., and Dan, K. (1972). Tension at the surface of the dividing sea-urchin egg. *J. Exp. Biol.* 57, 575–587.

Zhang, W., and Robinson, D.N. (2005). Balance of actively generated contractile and resistive forces controls cytokinesis dynamics. *Proc. Natl. Acad. Sci. USA* 102, 7186–7191.

## STAR★METHODS

### KEY RESOURCES TABLE

REAGENT or RESOURCE	SOURCE	IDENTIFIER
<b>Bacterial and virus strains</b>		
mCh-alpha-tubulin	Addgene	Cat#49149; RRID: Addgene 49149
pCMV/pCAG-LifeAct plasmids	Ibidi	Cat#60101
<b>Chemicals, peptides, and recombinant proteins</b>		
Cytochalasin B	Solarbio	Cat#C8080
Concanavalin A	Solarbio	Cat#C8110
Concanavalin A, Alexa Fluor 594 conjugate	Invitrogen	Cat#C11253
FITC-phalloidin	Beyotime	C2201S
Lipo8000	Beyotime	C0533
<b>Experimental models: Cell lines</b>		
HeLa cells	ATCC	CCL-2
<b>Software and algorithms</b>		
Prism8	GraphPad Software	<a href="http://www.graphpad.com">www.graphpad.com</a>
ImageJ	National Institutes of Health	<a href="https://imagej.nih.gov/ij/">https://imagej.nih.gov/ij/</a>

### RESOURCE AVAILABILITY

#### Lead contact

Further information and requests for resources and reagents should be directed to the lead contact, Prof. Fan Song ([songf@lnm.imech.ac.cn](mailto:songf@lnm.imech.ac.cn)).

#### Materials availability

This study did not generate new unique reagents.

#### Data and code availability

Any additional information required to reanalyze the data reported in this paper is available from the lead contact upon request.

### EXPERIMENTAL MODEL AND SUBJECT DETAILS

#### Cell lines

HeLa cells are cultured at 37°C in Dulbecco's modified Eagle medium (DMEM; Solarbio, China) supplemented with 10% fetal bovine serum (Solarbio, Australia origin) in a humidified incubator with 5% CO<sub>2</sub>.

### METHOD DETAILS

#### Solution exchange assay

To change the extracellular media, we use the device as shown in [Figure S8](#). One of the two injection pumps is used to extract the original media and the other is used to inject experimental media that have been pre-heated to 37°C. With the device, the time to exchange the solution is controlled within 20 s. The media with different osmolarities are obtained by mixing the normal medium (300 mOsm/kg) with sucrose solutions.

#### Local cytochalasin B delivery

We employ the BioPen system (Fluicell, Sweden) provided by Longfubiotech (China) to conduct the local delivery of cytochalasin B. The osmolarity of the delivery solution is regulated to be isotonic to avoid osmotic shock to cells.

### Cell labeling and imaging

Lifeact-GFP is purchased from Ibidi (Germany) and mCherry- $\alpha$ -tubulin is a gift from Gia Voeltz (Addgene plasmid # 49149; <http://n2t.net/addgene:49149>; RRID: Addgene 49149). Lipo8000 (Beyotime, China) is used for transfection of plasmid in HeLa cells. We use the EVOS FL Auto imaging system (Invitrogen, America) located in a MAWORDE workstation (Longfubiotech, China) to collect images. Live cell imaging of cells undergoing cytokinesis is performed in a humid atmosphere with 5% CO<sub>2</sub> at 37°C, using a 60 × NA 0.9 water objective (Olympus, Japan). To obtain the actin distribution at the end of cytokinesis, cells are fixed with 4% paraformaldehyde and permeabilized with 0.1% Triton-100 followed by staining of actin with FITC-phalloidin (Beyotime, China). Immunofluorescence image series are acquired from Z-stacks with a step of 0.366 μm using a 100 × NA 1.4 oil objective (Olympus, Japan). The images are processed using ImageJ.

### Cell volume calculation

We replace the isotonic media with hypotonic or hypertonic media when cells just enter into cytokinesis ( $C_f \approx 1$ ) and obtain the volumetric change based on the image series when the cell volume determined based on the spherical cap model becomes maximum or minimum. More specifically, the volume of the cell undergoing cytokinesis is determined by

$$V = \sum_{i=1,2} -\frac{2}{3}\pi R_i^3 + 2\pi R_i^2 \sqrt{R_i^2 - r^2} + \pi R_i r^2 + \frac{1}{3}\pi \left( R_i - \sqrt{R_i^2 - r^2} \right)^3 \quad (\text{Equation 7})$$

### Laplace pressure calculation

The Laplace pressure of cells undergoing cytokinesis is measured by micropipette aspiration. Micropipettes are pulled from glass capillaries to a diameter of 4–5 μm using a pipette puller (Narishige, Japan). The micropipette tip is bent to allow it to approach the cell at a very shallow angle, as close to horizontal as possible. The micropipette is filled with medium with 70% PBS and 30% serum before mounted on the micromanipulator (WPI, America). A cell is gently aspirated into the micropipette by applying negative low pressure  $p_i$ . For a general case, we can gradually decrease the pressure until it reaches the threshold value, at which the cell forms a hemispherical protrusion into the micropipette (Tinevez et al., 2009). Then the tension  $\tau$ , which is often assumed to be a constant using micropipette aspiration, can be calculated by  $\tau = (p_e - p_i)/[2(1/R_p - 1/R_c)]$  according to the Laplace law (Tinevez et al., 2009). Here,  $p_e$  is the pressure in the medium,  $R_p$  and  $R_c$  are the radii of the micropipette and the cell in contact with micropipette, respectively. On this basis, the Laplace pressure  $\Delta p$  of a cell is determined as  $\Delta p = 2\tau/R_c$ . In contrast, the Laplace pressure varies with time for cells undergoing cytokinesis. To measure the change of the Laplace pressure for cells undergoing cytokinesis in hypotonic or hypertonic media, we need to change the negative pressure to make the protrusion in the micropipette to be roughly hemispherical in shape, as similarly done in Ohtsubo and Hiramoto (1985). Then the change of Laplace pressure is determined when the Laplace pressure reaches maximum or minimum for hypotonic or hypertonic media in our study.

### $C_f$ calculation, bleb size and counting

To count bleb numbers, image series are acquired each 15s and  $C_f$  values are computed based on its definition. The  $C_f$  values that are closest to 0.2, 0.4, 0.6, and 0.8 are marked and rounded as nodes for stage partition. The size of a bleb is determined by calculating its projected area, which reaches a maximum when the bleb starts to retract. We can then obtain the maximum ratio of the projected area of blebs observed during cytokinesis to that of cells based on the image series. This maximum ratio  $S_B = \text{Max}(A_{bi}/A_{Cell})$  is defined as the relative bleb size, as illustrated in the schematic diagram of Figure 2B. We count continuously the number of blebs observed throughout the entire process of cytokinesis. Each bleb forming along the peripheries is successively assigned a number and is tracked until it vanishes. Then the maximum number assigned to blebs when the contractile-ring contraction completes is the total number of blebs observed during cytokinesis. If the duration of a bleb spans the different stages of cytokinesis, the bleb is assigned to the stage that the bleb just forms.

### QUANTIFICATION AND STATISTICAL ANALYSIS

Statistical analyses are performed using GraphPad Prism 8. Statistical Significance is assessed by Mann-Whitney test or two-way ANOVA followed by Tukey's test where appropriate. Significance levels are set to  $P = 0.05$ .